Arch. Metall. Mater. **71** (2026), 1, 151-156

DOI: https://doi.org/10.24425/amm.2026.157777

SHIH-HANG CHANG[1*]

COLD-ROLLING EFFECT ON LOW-FREQUENCY DAMPING PROPERTIES OF AZ31 MAGNESIUM ALLOY PLATE AT MODERATELY HIGH TEMPERATURE

This study investigated the influence of cold-rolling on the damping capacity of the hot-extruded AZ31 alloy plate. The damping capacity of the hot-extruded and the cold-rolled AZ31 alloy plates were measured by a dynamic mechanical analysis with a single cantilever from 0°C to 250°C at a constant heating rate. Experimental results demonstrated increased damping capacity, which is evident in both the P_2 peak and the high-temperature damping background (HTDB). The activation energy of the HTDB decreased from 2.01 eV to 0.91 eV after cold-rolling. This reduction suggests that the cold-rolling process accelerates grain boundary diffusion, promoting creep deformation at elevated temperatures. While cold-rolling enhances the HTDB damping capacity of the AZ31 alloy plate, it concurrently compromises its creep resistance at moderately high temperatures (100°C to 250°C). Therefore, for engineering applications of AZ31 alloy plates within this temperature range, careful consideration of this trade-off between improved damping and diminished creep resistance is crucial.

Keywords: AZ31 alloy; damping capacity; cold-rolling; high-temperature damping background; creep resistance

1. Introduction

Magnesium, with a density of 1.74 g/cm^3, is the lightest structural metal, and this property is regarded as the most important factor in the selection and use of many engineering designs. Numerous studies reported that magnesium and magnesium alloys could absorb energy during damping and are candidates for high-damping applications [1-8]. The damping capacities of magnesium and magnesium alloys at room temperature depend on the strain amplitude and relate to the movement of the dislocations in which the dislocations are weakly pinned by impurity atoms on the basal planes [9]. Despite their potential, the damping applications of magnesium alloys remain limited. This is because most alloying elements that increase strength tend to reduce their damping capacity [10,11]. Consequently, enhancing the damping capacity of magnesium alloys while maintaining their strength is crucial and a subject of extensive research. Several studies have demonstrated that incorporating reinforcements into magnesium alloys to create composites can substantially enhance their damping capacity [12-16]. Additionally, the literature suggests that magnesium and its alloys can exhibit enhanced damping properties when fabricated into porous structures or subjected to specific thermomechanical treatments or microstructural control [17-19].

Recently, Su et al. stated that pure magnesium's damping and mechanical properties can be balanced by grain refinement to sub-micron and nanometer scales [20]. Wang et al. [21] provided a novel method for preparing high-strength and high-damping capacity Mg alloys by ultra-high pressure technology [22,23]. Bian et al. [24] reported that Mg–0.03Cu–0.05Ca alloy exhibited superior damping performance than AZ31 alloy but lower than pure Mg as the solute segregation at grain boundaries. Huang et al. [25] reported that the mechanical properties and internal friction of Mg-Li alloys could be enhanced under high-temperature and high-pressure conditions because of the formation of a supersaturated solid solution, notable grain size refinement, the introduction of large amounts of nanoscale twins, and the precipitation of spherical secondary phases.

Most of the literature only focused on the damping characteristics of magnesium alloys at room temperature. However, it is necessary to understand the information on the damping properties of magnesium alloys at room temperature and moderately high temperatures because the strength of magnesium alloys rapidly drops at those temperatures [10,11]. According to our previous studies [25-28], the microstructures and thermomechanical treatments influence magnesium alloys' damping properties at moderately high temperatures. The damping properties of magnesium alloys at moderately high temperatures are as-

[1] NATIONAL I-LAN UNIVERSITY, DEPARTMENT OF CHEMICAL AND MATERIALS ENGINEERING, I-LAN 260, TAIWAN

* Corresponding author: shchang@niu.edu.tw

sociated with grain boundary sliding [5], which also corresponds to the creep behavior of magnesium alloys. Given the critical importance of mechanical properties at moderately elevated temperatures for practical applications of magnesium alloys, this study investigates the damping capacity of hot-extruded and/or cold-rolled AZ31 alloy plate over a temperature range of 0°C to 250°C using dynamic mechanical analysis (DMA). The primary objective is to understand cold-rolling's influence on the damping characteristics and creep resistance of the AZ31 alloy plate.

2. Experimental

AZ31 alloy with an 8"-diameter billet was purchased from MEL Chemicals, a division of Magnesium Elektron Ltd, England. The billet was then hot-extruded at 300°C to become 1.38 mm thickness plates at 2 m min^{-1} extrusion speed. Four hot-extruded AZ31 alloy plates were cut and cold-rolled at room temperature to 1.05 mm thick with 24% thickness reduction, followed by annealing at 100°C for 10 min. The specimens of the AZ31 alloy plates for the microstructural examination were prepared by the standard metallographic procedure with the etching solution of 7 ml alcohol + 1 ml picric acid + 1 ml acetic acid + 1 ml deionized water. Microstructural observations of the AZ31 alloy plates were performed with a Nikon FX-35DX optical microscope (OM). The tan δ, which is defined as the ratio of the loss modulus to the storage modulus, of the hot-extruded and the cold-rolled AZ31 alloy plates were measured by TA 2980 DMA equipment with a single cantilever from 0°C to 250°C at a constant heating rate of 3°C min^{-1}. The size of the DMA specimen was 30 mm in length and 12 mm in width, and its longitudinal direction was along the extrusion and cold-rolling direction. The testing frequencies were set at 0.1, 0.5, 1, and 5 Hz. The strain amplitude was set at 20 μm.

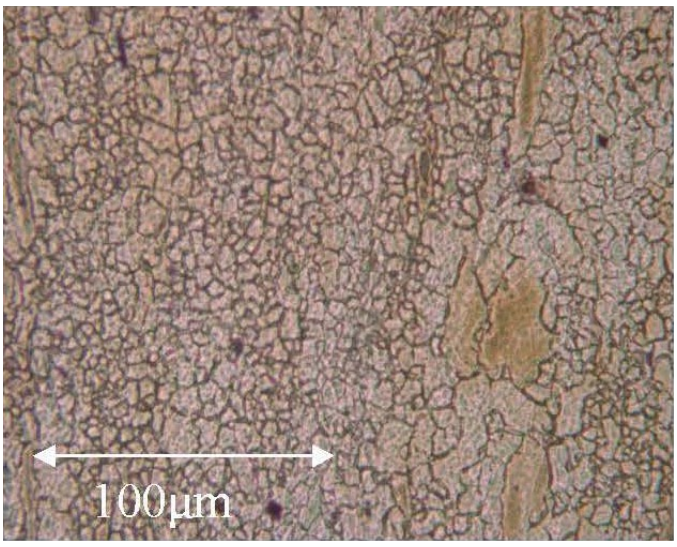

(a)

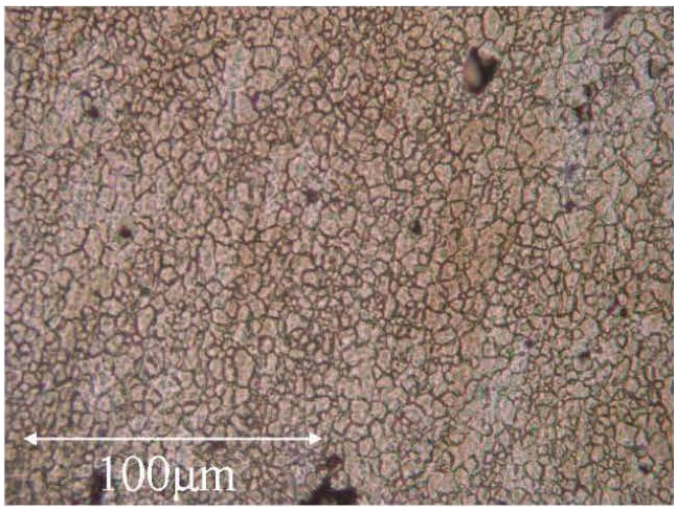

(b)

Fig. 1. Optical microscope images of (a) as hot-extruded and (b) after cold-rolled and annealed (100°C for 10 min) AZ31 alloy plates observed by optical microscopy

3. Results and discussion

3.1. Cold-rolling effect on the microstructures and damping capacities of AZ31 alloy plates

Figs. 1(a) and 1(b) show the microstructures, observed by optical microscopy, of the hot-extruded and the cold-rolled AZ31 alloy plate, respectively. According to Fig. 1, the grain size of the hot-extruded AZ31 alloy plate is calculated as approximately 10 μm. The grain size of the AZ31 alloy plate was slightly reduced to approximately 7.6 μm after the cold-rolling process.

Fig. 2 shows the heating curve of tan δ versus temperature for hot-extruded and cold-rolled AZ31 alloy plate measured at 1 Hz frequency and 20 μm amplitude (strain = 2.5×10^{-4}) from 0°C to 250°C. As shown in Fig. 2, the heating tan δ curve exhibits two internal friction peaks, P_1 and P_2, at approximately 60°C and 170°C, respectively. Similar results have also been observed in pure Mg (99.96 wt.%) and Mg-Ni alloys (6.2 ~ 22.6 wt.% Ni) [6]. In these materials, the P_1 peak is attributed to dislocation movement on the basal planes, while the P_2 peak is attributed to grain boundary sliding. Apart from P_1 and P_2 peaks shown in Fig. 2, the heating tan δ curve can be divided into an athermal internal friction background (for temperature below 100°C) and an exponential internal friction background (for temperature above 100°C). The exponential internal friction background is also termed as high-temperature damping background (HTDB) and has been observed in many alloys and intermetallics [29-31]. However, the detailed damping mechanism of HTDB for AZ31 alloy plate has not been systematically studied. Fig. 2 also shows the heating curve of tan δ versus temperature for cold-rolled AZ31 alloy plate measured at 1 Hz frequency and 20 μm amplitude (strain = 2.5×10^{-4}) from 0°C to 250°C. Fig. 2 shows that the variation of the P_1 peak is inconspicuous after cold-rolling, while the tan δ values of both the P_2 peak and HTDB increase. This feature implies that the high-temperature damping capacity of AZ31 alloy plate can be improved by cold-rolling.

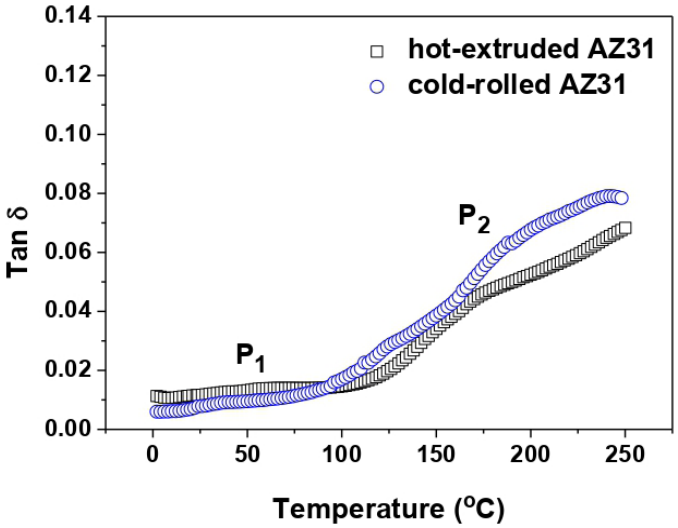

Fig. 2. The tan δ values vs. temperature for hot-extruded and cold-rolled AZ31 alloy plates measured by DMA at a frequency of 1 Hz

Figs. 3(a) and 3(b) show the heating tan δ curves of the hot-extruded and the cold-rolled AZ31 alloy plate, respectively, measured at 20 μm amplitude with various frequencies (from 0.1 Hz to 5 Hz). As shown in Figs. 3(a) and 3(b), the P_1 peak of the cold-rolled AZ31 alloy plate is located around the room temperature, and its tan δ value is slightly lower than that of the hot-extruded one. This is because the strain amplitude for as hot-extruded AZ31 alloy plate (strain = 2.5×10^{-4}) is slightly larger than that for the cold-rolled one (strain = 1.9×10^{-4}) since the former thickness is thicker than the latter one. However, at temperatures above 100°C, the tan δ value of the cold-rolled AZ31 alloy plate becomes much larger than that of the as hot-extruded one in each testing frequency. This indicates that the cold-rolling effect becomes dominant around P_2 peak and HTDB, which are located at temperatures above 100°C. In addition, also from Figs. 3(a) and 3(b), the P_2 peak temperatures of hot-extruded and cold-rolled AZ31 alloy plates both shift to higher temperatures with increasing frequency. This feature implies that the P_2 peak exhibits a relaxation characteristic and is thermally activated. However, it is not easy to separate the ill-defined P_2 peak precisely from the HTDB. Further study on the damping property of P_2 peak with more appropriate analysis is still conducting in our future research.

3.2. Cold-rolling effect on the HTDB of AZ31 alloy plates

Fig. 3(a) demonstrates that the tan δ value of the hot-extruded AZ31 alloy plate increases with decreasing frequency at a constant temperature. This frequency dependence of tan δ indicates viscoelastic behavior in the as-hot-extruded AZ31 alloy plate. The ideal viscoelastic relaxation behavior can be modeled using a Maxwell rheological model. In dynamic experiments, the internal friction can be described as [30]:

$$Q^{-1} = \tan\delta = 1/\omega\tau \quad (1)$$

where ω is the circular frequency and τ is the relaxation time. However, Eq. (1) is inadequate for accurately describing the behavior of real viscoelastic materials. This is because real materials exhibit a distribution of relaxation times. To account for this, the empirical spectrum parameter 'n' is introduced into Eq. (1) [32].

$$Q^{-1} = 1/(\omega\tau)^n \quad (2)$$

where $0 \le n \le 1$ ($n = 1$ for "ideal" viscoelasticity). Since viscoelastic behavior at high temperatures can be determined by the thermally activated process, an Arrhenius equation holds for the relaxation time τ [33]:

$$\tau = \tau_0 \exp(H/kT) \quad (3)$$

where τ_0 is the limit relaxation time, H is the activation energy, k is the Boltzmann's constant and T is the temperature. For the

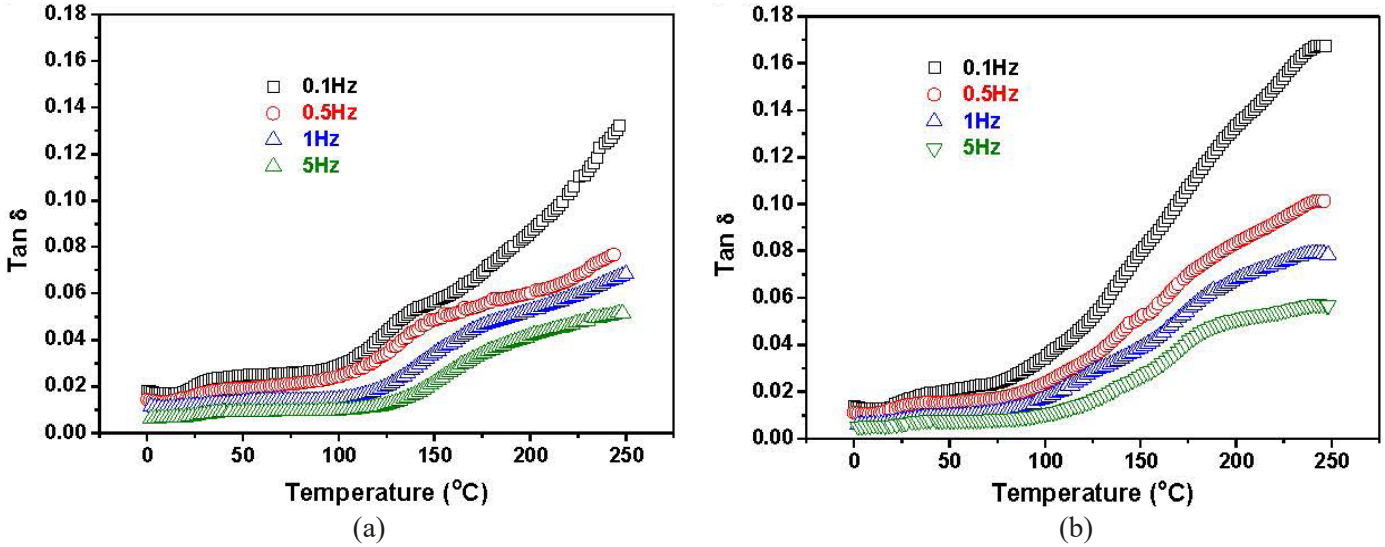

Fig. 3. (a) Tan δ curves for as hot-extruded AZ31 alloy plate measured with different frequencies from 0.1 Hz to 5 Hz. (b) Tan δ curves for as cold-rolled AZ31 alloy plate measured with different frequencies from 0.1 Hz to 5 Hz

analysis of the HTDB, it is convenient to use the logarithmic representation of Eq. (2):

$$\ln Q^{-1}(T,\omega) = -n\ln\omega - n\ln\tau(T) \quad (4)$$

Fig. 4(a) shows the logarithmic plot ($\ln Q^{-1}$ versus $\ln\omega$ for various temperatures) of the HTDB data which are determined from Fig. 3(a) at different temperatures above 190°C. As seen in Fig. 4(a), the measured $\ln Q^{-}$ and $\ln\omega$ shows a linear dependence, which is in accordance with the expectation of the viscoelastic relaxation behavior. From the slope and intercept of the fitting lines shown in Fig. 4(a), the n value and the relaxation time τ measured at each temperature can be determined. Fig. 4(b) plots the relaxation time τ as a function of temperature in which τ was measured from various temperatures in Fig. 4(a). From Fig. 4(b), the activation energy of the HTDB for as hot-extruded AZ31 alloy plate can be determined from the slope of the fitting line as the value of H = 2.01 eV. Fig. 5(a) plots the logarithmic plot ($\ln Q^{-}$ versus $\ln\omega$ for various temperatures) of the HTDB data, which are determined at different temperatures above 190°C in Fig. 3(b) for the cold-rolled AZ31 alloy plate. Fig. 5(b) shows the relaxation time τ measured from Fig. 5(a) as a function of temperature. From Fig. 5(b), the calculated activation energy of the HTDB for cold-rolled AZ31 alloy plate is H = 0.91 eV.

Many studies reveal that the HTDB possesses viscoelastic nature and is only present in polycrystalline materials [34,35]. Therefore, it is reasonable to suggest that the HTDB is associated with creep behavior, which also possesses viscoelastic characteristic at high temperature [34]. This study observed a significant decrease in the activation energy of the HTDB for AZ31 alloy plate from 2.01 eV to 0.91 eV following cold-rolling. This reduction indicates that the cold-rolling process accelerates grain boundary diffusion, thereby promoting creep development

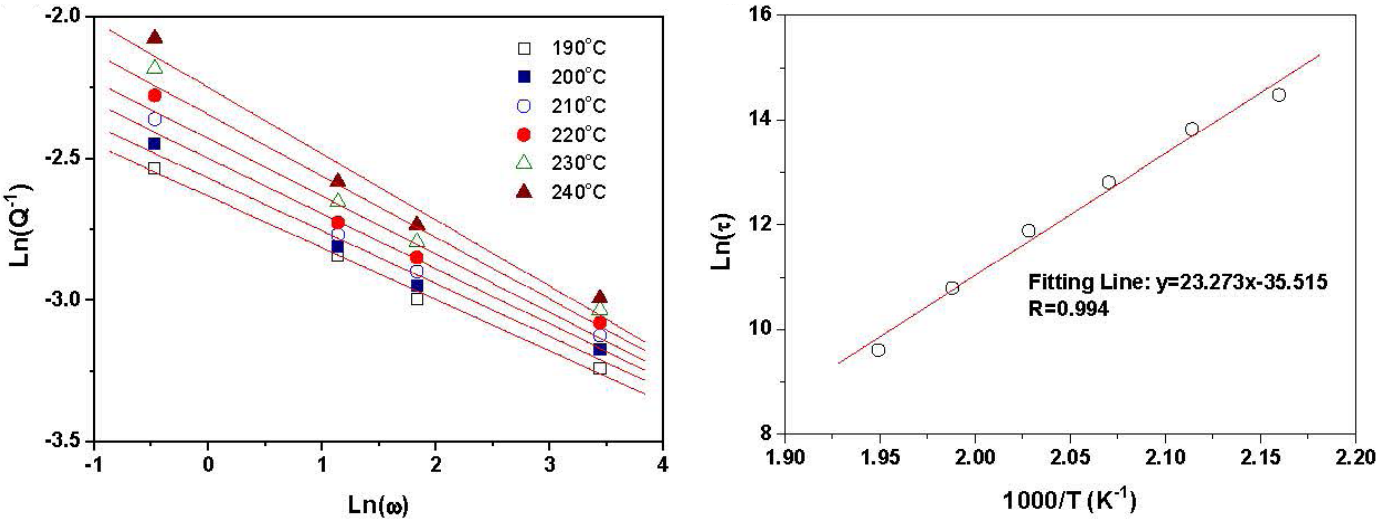

(a) (b)

Fig. 4. (a) The plot of $\ln Q^{-1}$ versus $\ln\omega$ for various temperatures measured from Fig. 3(a). (b) Arrhenius plot ($\ln\tau$ versus $1/T$) determined from (a) for as hot-extruded AZ31 alloy plate

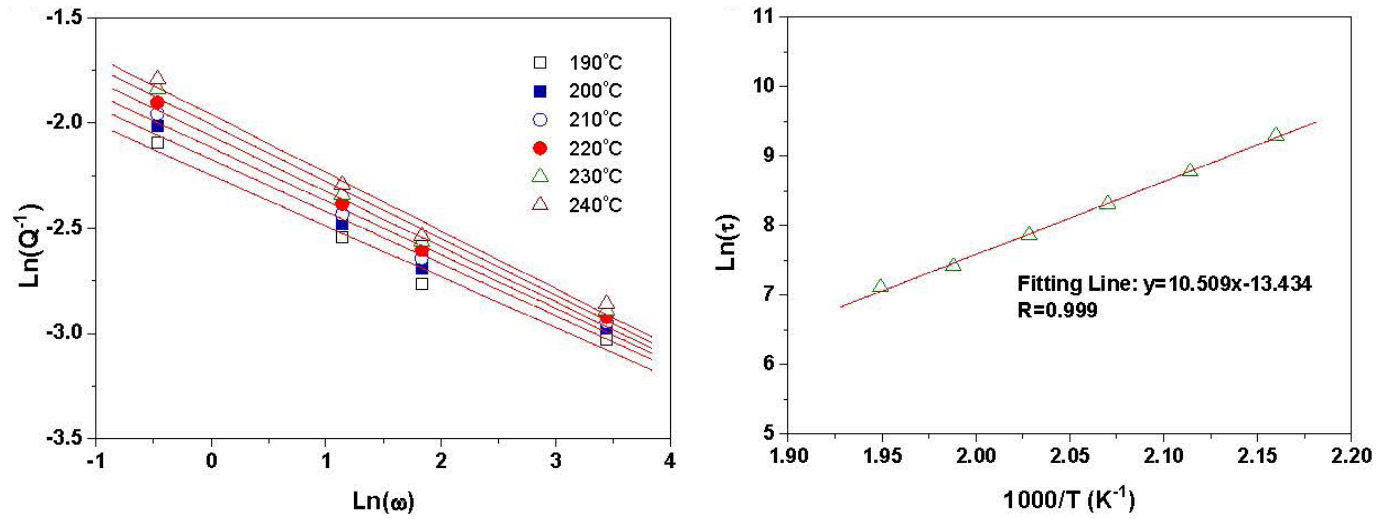

(a) (b)

Fig. 5. (a) The plot of $\ln Q^{-1}$ versus $\ln\omega$ for various temperatures measured from Fig. 3(b). (b) Arrhenius plot ($\ln\tau$ versus $1/T$) determined from (a) for cold-rolled AZ31 alloy plate

at elevated temperatures. In essence, while cold-rolling effectively enhances the HTDB damping capacity of the AZ31 alloy plate, it concurrently compromises its creep resistance at high temperatures. Therefore, a careful consideration of this trade-off between enhanced damping and diminished creep resistance is crucial for optimizing the mechanical and damping performance of AZ31 alloy plate in moderately high-temperature applications.

3.3. Annealing effect on damping characteristics of cold-rolled AZ31 alloy plates

Fig. 6 presents heating tan δ curves as a function of temperature for AZ31 alloy plates subjected to cold-rolling followed by annealing at 100°C for varying durations (1 to 6 hours). The heating tan δ curve of the as-cold-rolled AZ31 alloy plate (from Fig. 2) is also included for comparison. All measurements in Fig. 6 were conducted at a frequency of 1 Hz, an amplitude of 20 μm, and a heating rate of 3°C min^{-1} from 0°C to 250°C. As evident in Fig. 6, the tan δ values of the specimens after cold-rolling, regardless of annealing time, remaining essentially unchanged. This observation suggests that annealing at 100°C has a negligible effect on the damping capacity of the cold-rolled AZ31 alloy plate.

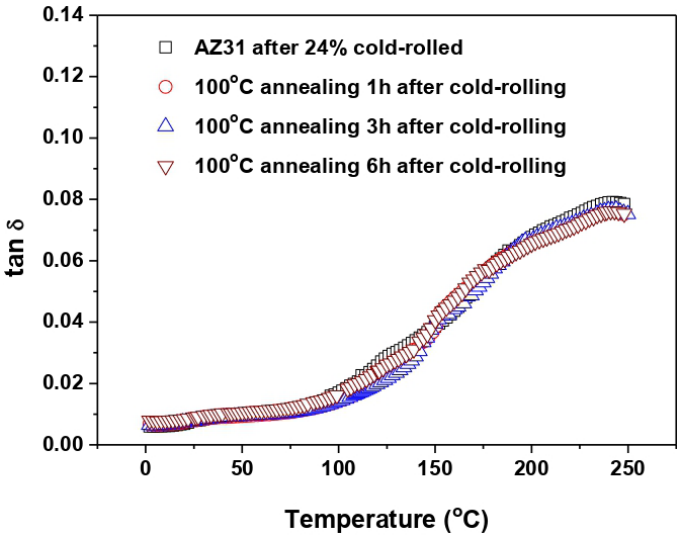

Fig. 6. The tan δ values vs. temperature for as cold-rolled and annealed AZ31 alloys measured by DMA at a frequency of 1 Hz

4. Conclusions

In this study, we investigated the effect of cold rolling on the damping capacity and the HTDB of the hot-extruded AZ31 alloy plates. The following conclusions were drawn.

1. The grain size of the hot-extruded AZ31 alloy plate gradually decreased from approximately 10 μm to approximately 7.6 μm after the cold-rolling process.
2. The P_2 peak, which is attributed to grain boundary sliding, exhibited a relaxation characteristic and is thermally activated. The damping capacity of the P_2 peak was increased after the cold-rolling process.
3. The damping capacity of the HTDB for the AZ31 alloy plate increased after cold-rolling, while the activation energy of the HTDB decreased significantly from 2.01 eV to 0.91 eV simultaneously.
4. The cold-rolling process improved the damping capacity of the AZ31 alloy plate but also accelerated the grain boundary diffusion, thereby facilitating creep at moderately high temperatures.

Acknowledgment

The author gratefully acknowledges the financial support for this research provided by the National Science and Technology Council (NSTC), Taiwan, under Grant NSTC 112-2221-E-197-014-MY2.

REFERENCES

[1] J. Wang, Z. Wan, C. Dang, Y. Zou, J. Wang, F. Pan, Materials **16** (23), 7318 (2022). DOI: https://doi.org/10.3390/ma16237318

[2] K. Kim, Y. Ji, K. Kim, M. Park, Materials **16** (4), 1399 (2022). DOI: https://doi.org/10.3390/ma16041399

[3] A. Anilchandra, M. Surappa, Mater. Sci. Eng. A **542**, 94-103 (2012). DOI: https://doi.org/10.1016/j.msea.2012.02.038

[4] O. Lambri, W. Riehemann, Z. Trojanová, Scr. Mater. **45** (12), 1365-1371 (2001). DOI: https://doi.org/10.1016/S1359-6462(01)01171-X

[5] H. Watanabe, T. Mukai, M. Sugioka, K. Ishikawa, Scr. Mater. **51** (4), 291-295 (2004). DOI: https://doi.org/10.1016/j.scriptamat.2004.04.032

[6] X. Hu, Y. Zhang, M. Zheng, K. Wu, Scr. Mater. **52** (11), 1141-1145 (2005). DOI: https://doi.org/10.1016/j.scriptamat.2005.01.048

[7] C. Zhao, F. Wang, J. Li, J. Zeng, S. Dong, F. Wang, L. Jin, J. Dong, Scr. Mater. **240**, 115845 (2024). DOI: https://doi.org/10.1016/j.scriptamat.2023.115845

[8] C. Dang, J. Wang, J. Wang, D. Yu, W. Zheng, C. Xu, R. Lu, J. Mater. Res. Technol. **22**, 2589-2599 (2022). DOI: https://doi.org/10.1016/j.jmrt.2022.12.087

[9] K. Sugimoto, K. Matsui, T. Okamoto, K. Kishitake, Mater. Trans. JIM **16** (10), 647-656 (1975). DOI: https://doi.org/10.2320/matertrans1960.16.647

[10] K. Suzuki, Y. Chino, X. Huang, M. Mabuchi, Mater. Trans. **52** (10), 2040-2044 (2011). DOI: https://doi.org/10.2320/matertrans.M2011184

[11] K. Hazeli, A. Sadeghi, M.O. Pekguleryuz, A. Kontsos, Mater. Sci. Eng. A **589**, 275-279 (2014). DOI: https://doi.org/10.1016/j.msea.2013.09.090

[12] Y.W. Wu, K. Wu, K.K. Deng, K.B. Nie, X.J. Wang, X.S. Hu, M.Y. Zheng, Mater. Sci. Eng. A **527** (26), 6816-6821 (2010). DOI: https://doi.org/10.1016/j.msea.2010.07.050

[13] K.K. Deng, J.C. Li, K.B. Nie, X.J. Wang, J.F. Fan, Mater. Sci. Eng. A **624**, 62-70 (2015). DOI: https://doi.org/10.1016/j.msea.2014.11.069

[14] C.J. Wang, K.K. Deng, W. Liang, Mater. Sci. Eng. A **668**, 55-58 (2016). DOI: https://doi.org/10.1016/j.msea.2016.05.055

[15] W.Z. Huang, H.J. Luo, Y.L. Mu, H. Lin, H. Du, Int. J. Miner. Metall. Mater. **24**, 701-707 (2017). DOI: https://doi.org/10.1007/s12613-017-1453-y

[16] Q. Li, J. Li, G. He, Mater. Sci. Eng. A **680**, 92-96 (2017). DOI: https://doi.org/10.1016/j.msea.2016.10.089

[17] Q. Li, G. Jiang, J. Dong, J. Hou, G. He, J. Alloys Compd. **680**, 522-530 (2016). DOI: https://doi.org/10.1016/j.jallcom.2016.04.101

[18] H. Somekawa, H. Watanabe, D.A. Basha, A. Singh, T. Inoue, Scr. Mater. **129**, 35-38 (2017). DOI: https://doi.org/10.1016/j.scriptamat.2016.10.019

[19] L.B. Ren, G.F. Quan, Y.G. Xu, D.D. Yin, J.W. Lu, J.T. Dang, J. Alloys Compd. **699**, 976-982 (2017). DOI: https://doi.org/10.1016/j.jallcom.2016.12.299

[20] D. Su, J. Fan, Q. Zhang, H. Dong, Mater. Sci. Eng. A **931**, 148208 (2025). DOI: https://doi.org/10.1016/j.msea.2025.148208

[21] D. Wang, P. Huang, R. Wu, H. Huang, T. Zhong, C. Zou, Y. Song, J. Rare Earths **42**, 2279-2284 (2024). DOI: https://doi.org/10.1016/j.jre.2024.07.029

[22] D. Wang, P. Huang, R. Wu, H. Huang, R. Yu, M. Sang, L. Peng, Y. Song, Y. Jin, Y. Liu, Z. Zhou, Mater. Sci. Eng. A **915**, 147205 (2024). DOI: https://doi.org/10.1016/j.msea.2024.147205

[23] M. Bian, X. Huang, Y. Chino, J. Alloys Compd. **1010**, 177215 (2025). DOI: https://doi.org/10.1016/j.jallcom.2024.177215

[24] P. Huang, M. Sang, D. Wang, H. Huang, R. Wu, X. Yang, Y. Han, R. Yu, L. Zhang, J. Alloys Compd. **1022**, 179877 (2025). DOI: https://doi.org/10.1016/j.jallcom.2025.179877

[25] S.K. Wu, S.H. Chang, T.Y. Chou, S. Tong, J. Alloys Compd. **465** (1-2), 210-215 (2008). DOI: https://doi.org/10.1016/j.jallcom.2007.10.134

[26] S.H. Chang, S.K. Wu, W.L. Tsai, J.Y. Wang, J. Alloys Compd. **487** (1-2), 142-145 (2009). DOI: https://doi.org/10.1016/j.jallcom.2009.08.006

[27] S.K. Wu, S.H. Chang, W.L. Tsia, H.Y. Bor, Mater. Sci. Eng. A **528** (18), 6020-6025 (2011). DOI: https://doi.org/10.1016/j.msea.2011.04.047

[28] S.H. Chang, S.K. Wu, Y.H. Li, K.C. Lin, H.Y. Bor, Mater. Trans. **53**(2), 407-411 (2012). DOI: https://doi.org/10.2320/matertrans.M2011174

[29] P. Barrand, Acta Metall. **14** (10), 1247-1256 (1966). DOI: https://doi.org/10.1016/0001-6160(66)90242-2

[30] G. Haneczok, M. Weller, Mater. Sci. Eng. A **370** (1-2), 209-212 (2004). DOI: https://doi.org/10.1016/j.msea.2003.01.009

[31] M. Weller, H. Clemens, G. Haneczok, Mater. Sci. Eng. A **442** (1-2), 138-141 (2006). DOI: https://doi.org/10.1016/j.msea.2006.02.220

[32] G. Schöeck, E. Bisogni, E. Shyne, T Acta Metall. **12** (12), 1466-1468 (1964). DOI: https://doi.org/10.1016/0001-6160(64)90141-5

[33] C.Y. Xie, E. Carreño-Morelli, R. Schaller, Scr. Mater. **39** (2), 225-230 (1998). DOI: https://doi.org/10.1016/S1359-6462(98)00158-4

[34] M. Weller, A. Chatterjee, G. Haneczok, H. Clemens, J. Alloys Compd. **310**(1-2), 134-138 (2000). DOI: https://doi.org/10.1016/S0925-8388(00)00934-8

[35] M. Weller, A. Chatterjee, G. Haneczok, E. Arzt, F. Apple, H. Clemens, Z. Metallkd. **92** (8), 1019-1025 (2001). DOI: https://doi.org/10.1515/ijmr-2001-0183